

## Asymmetric hysteresis loop in magnetostatic-biased multilayer nanowires

This article has been downloaded from IOPscience. Please scroll down to see the full text article.

2009 Nanotechnology 20 445707

(<http://iopscience.iop.org/0957-4484/20/44/445707>)

[The Table of Contents](#) and [more related content](#) is available

Download details:

IP Address: 158.170.162.163

The article was downloaded on 07/10/2009 at 14:51

Please note that [terms and conditions apply](#).

# Asymmetric hysteresis loop in magnetostatic-biased multilayer nanowires

S Allende<sup>1,2</sup>, J Escrig<sup>1,3</sup>, D Altbir<sup>1,3</sup>, E Salcedo<sup>4</sup> and M Bahiana<sup>5</sup>

<sup>1</sup> Departamento de Física, Universidad de Santiago de Chile (USACH), Avenida Ecuador 3493, 917-0124 Santiago, Chile

<sup>2</sup> Departamento de Física, FCFM, Universidad de Chile, Casilla 487-3, Santiago, Chile

<sup>3</sup> Centro para el Desarrollo de la Nanociencia y Nanotecnología, CEDENNA, 917-0124 Santiago, Chile

<sup>4</sup> Instituto de Física, Universidade Federal do Rio Grande do Sul, CP 15051, 91501-970 Porto Alegre, RS, Brazil

<sup>5</sup> Instituto de Física, Universidade Federal do Rio de Janeiro, CP 68528, 21945-970 Rio de Janeiro, RJ, Brazil

E-mail: [juan.escrig@usach.cl](mailto:juan.escrig@usach.cl)

Received 3 June 2009, in final form 4 September 2009

Published 7 October 2009

Online at [stacks.iop.org/Nano/20/445707](http://stacks.iop.org/Nano/20/445707)

## Abstract

The hysteresis of multilayer nanowires composed by a soft magnetic cylindrical wire, a non-magnetic spacer layer and an external hard magnetic shell is investigated. The external magnetic shell originates a non-homogeneous magnetic field on the inner wire, which is responsible for a displacement and a change of the width of the hysteresis curve of the wire. Moreover, different reversal modes occur at each branch of the hysteresis loop, which can be understood by analyzing the interaction magnetostatic field along the wire. Our results open the possibility of controlling two parameters of the hysteresis loop, the coercivity and the bias, providing an interesting system to be investigated.

(Some figures in this article are in colour only in the electronic version)

## 1. Introduction

In recent years a great deal of attention has been focused on developing novel nanostructures which can be fundamental to future applications. In particular, patterned magnetic nanostructures such as arrays of wires, tubes, stripes or rings have been developed in order to be used in data storage, microelectronics or biomedical processes like cell separation or biosensing. Among the different types of nanostructures, tubes offer an additional degree of freedom as compared to nanowires, because not only the length and diameter can be varied, but also the thickness of the tube walls [1]. Other similar nano-objects are the multilayer microwires, introduced by Pirota *et al* [2], consisting of two metallic layers separated by an intermediate insulating microlayer. Different techniques, like quenching and drawing, sputtering and electroplating, have been combined to prepare these particles with controlled geometry. The synthesis of multilayer microwires, magnetic nanowires and nanotubes opens the possibility of fabricating multilayer nanowires where new magnetic properties can

appear since, depending on the geometry, the internal and external layers can be close enough to interact via a strong dipolar coupling [3]. This interaction is responsible for the appearance of interesting magnetic properties, such as the dipolar magnetic bias previously reported in microwires [4, 5]. In this paper we focus on this latter property, investigating, by means of numerical simulations, how the hysteresis loop bias varies as the outer layer thickness changes. Our results show that there exists a displacement and a change of the width of the hysteresis curve due to the magnetostatic field. Also we observe the existence of different reversal processes at each branch of the hysteresis curve, which can be understood by analyzing the non-homogeneous magnetostatic field along the wire due to the external tube.

## 2. Model

The system we have in mind consists of a multilayer wire composed by a cylindrical wire of soft magnetic material, a spacer layer made of non-magnetic material and an external

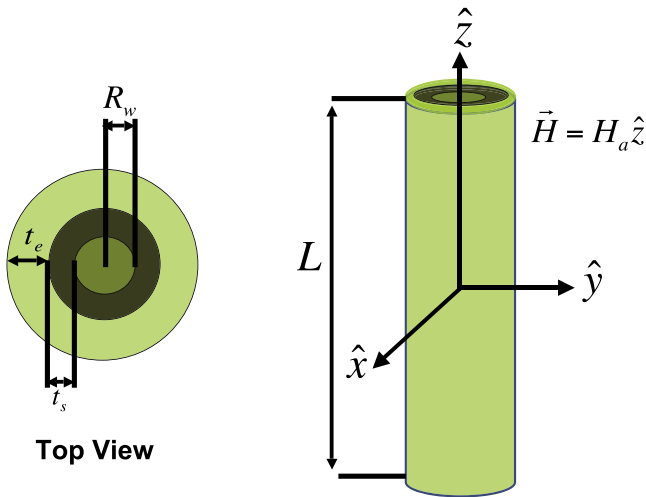


**Figure 1.** Definition of parameters of the geometry of the multilayer wire.

hard magnetic shell. In some experiments with multilayered microwires the spacer layer is usually made of Pyrex glass and a layer of gold, necessary for the addition of the outermost layer of hard magnetic material [2]. Figure 1 shows the definition of the important parameters in this geometry.

In this work we consider that the innermost layer is a uniform Ni nanowire with radius  $R_w = 15$  nm, built along the [001] direction of a fcc lattice with parameter  $a_0 = 3.52$  Å. The spacer layer has a width  $t_s = 15$  nm and the thickness  $t_e$  of the external magnetic layer, made of Co, ranges from 0 to 300 nm. The length of the multilayer particle is  $L = 500$  nm. Such a system contains about  $10^9$  atoms, which is out of reach for a regular Monte Carlo simulation with dipolar interactions, considering the available computational power. In order to reduce the number of interacting atoms we make use of a scaling technique, proposed by d'Albuquerque *et al* [6], originally formulated to investigate the equilibrium phase diagram of cylindrical particles of height  $h$  and diameter  $d$ . The authors showed that this diagram is equivalent to the one for a smaller particle with  $d' = d\chi^\eta$  and  $h' = h\chi^\eta$ , with  $\chi < 1$  and  $\eta \approx 0.56$ , if the exchange constant is also scaled as  $J' = \chi J$ . It has also been shown [7] that the scaling relations can be used together with Monte Carlo simulations to obtain the general magnetic state of a nanoparticle. We use this idea starting from the desired value for the total number of interacting particles we can deal with, based on the available computational facilities. As will be shown later, the atoms in the inner and outer shells have different roles in the simulations. We have estimated  $N \approx 1000$  for the inner wire, leading to the scale value  $\chi = 2.0 \times 10^{-3}$  and 903 magnetic moments. This scaling leads to an outer layer with 2000–500 000 magnetic moments, depending on the chosen value for  $t_e$ . In its original formulation, the scaling technique did not include temperature. However, since thermal activation is a key issue for transitions between metastable states and the energy landscape depends on the value of  $\chi$ , temperature must also be scaled. Temperature scaling is still an open issue. We considered that, even if the energy landscape is

rather complicated due to the dipolar interaction, in the vicinity of each local minimum we can analyze the transitions as regulated by simple energy barriers of the form  $K_e V_e$ , where  $K_e$  is an effective anisotropy constant taking into account several energy contributions, and  $V_e$  is an effective volume. Thermally activated transitions naturally lead to the definition of a blocking temperature  $T_B \propto K_e V_e$  [8], so we use this idea to relate temperature and size. In order to keep the thermal activation process invariant under the scaling transformation, the energy barriers must also be invariant; therefore, the temperature should scale as the volume, that is,  $T' = \chi^{3\eta} T$ . This technique was presented by Vargas *et al* [7] and has been used before to investigate magnetic dots [9], tubes [10], and wires [11], showing good agreement with experiments and micromagnetic calculations.

Our goal is to examine the reversal process of the inner wire, subject to the magnetostatic field of the external layer. Usually experiments of this kind involve a premagnetization process, in which a field near the saturation value for the outer shell is applied. The hysteresis loops are then obtained by varying the external field within limits much lower than the premagnetizing field [2]. Therefore, a reasonable approximation is to consider that the outer shell does not change during the reversal process of the soft nucleus. The spacer layer thickness is chosen such that exchange coupling between the two magnetic layers can be safely neglected.

In this picture we write the energy of the  $\alpha$ th magnetic moment in the wire as

$$E_\alpha = -\vec{m}_\alpha \cdot \vec{B}_\alpha = -\vec{m}_\alpha \cdot \mu_0 \vec{H}_\alpha, \quad (1)$$

where  $\vec{H}_\alpha$  is the effective field acting on  $\vec{m}_\alpha$ , including contributions from the applied field ( $\vec{H}_a$ ), exchange of the inner wire ( $\vec{H}_x = J \sum_{j \in \{\text{nn}\}} \vec{m}_j$ ), magnetostatic field within the wire ( $\vec{H}_m^w = \sum_{j \in \{\text{w}\}} \frac{3(\vec{m}_j \cdot \hat{n}_{\alpha j}) \hat{n}_{\alpha j} - \vec{m}_j}{r_{\alpha j}^3}$ ) and the magnetostatic field generated by the external layer ( $\vec{H}_m^e = \sum_{j \in \{\text{e}\}} \frac{3(\vec{m}'_j \cdot \hat{n}_{\alpha j}) \hat{n}_{\alpha j} - \vec{m}'_j}{r_{\alpha j}^3}$ ), in the form

$$\vec{H}_\alpha = \vec{H}_a + \vec{H}_x + \vec{H}_m^w + \vec{H}_m^e, \quad (2)$$

where  $J$  is the exchange coupling constant,  $\{\text{nn}\}$  the set of nearest neighbors of  $\alpha$ ,  $\{\text{e}\}$  the set of magnetic moments in the external layer,  $\{\text{w}\}$  the set of magnetic moments in the inner wire,  $r_{\alpha j}$  the distance to the  $j$ th atom, and  $\hat{n}_{\alpha j}$  the unitary vector along  $\vec{r}_{\alpha j}$ . According to our assumption the term corresponding to  $\vec{H}_m^e$  does not vary in time and has to be calculated only once. For the hard outer layer we assume that  $m' = 1.71 \mu_B$ , corresponding to cobalt. For the wire we take the saturation value of nickel, that is  $m = 0.615 \mu_B$ . The corresponding value for the exchange coupling constant of Ni is  $J = 1600$  kOe/ $\mu_B$  [12, 13].

Monte Carlo simulations were carried out at  $T = 300$  K, using the Metropolis algorithm [14] with the new orientation of the magnetic moments restricted according to the scheme proposed by Nowak *et al* [16]. Only the magnetic moments in the inner wire were considered for Monte Carlo moves. The initial state had  $H_a = 15$  kOe, higher than the saturation field, and all magnetic moments parallel to  $\vec{H}_a$ . The field was then linearly decreased until  $-5$  kOe and then increased at a rate

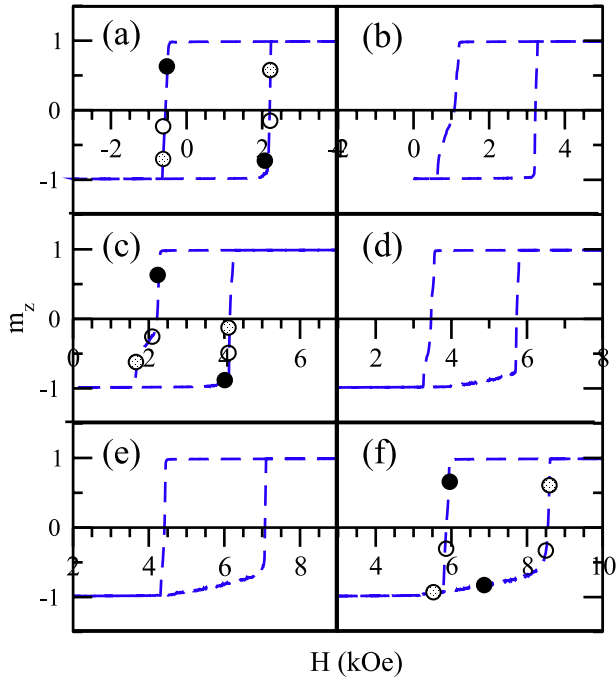


**Figure 2.** Hysteresis loops for (a)  $t_e = 10$  nm, (b)  $t_e = 50$  nm, (c)  $t_e = 90$  nm, (d)  $t_e = 150$  nm, (e)  $t_e = 200$  nm, and (f)  $t_e = 300$  nm.

of  $\Delta H_a = 0.01$  kOe for every 300 MC steps. In this way, about 200 000 MC steps are needed to go from saturation to the coercive field.

### 3. Results

Figure 2 illustrates the hysteresis loops of the internal wire for  $t_e = 10, 50, 90, 150, 200$  and  $300$  nm. The dots depict different moments along the reversal process which will be further investigated in detail. In this figure we observe that, as  $t_e$  is varied, the hysteresis loop is shifted towards positive fields, presents variations in its width and becomes non-symmetric, evidencing the existence of different reversal modes at each branch.

In order to quantify the shift, or bias, of the hysteresis loop, we define the bias field,  $H_b$ , in terms of the coercive fields at the right and left branches,  $H_{c+}$  and  $H_{c-}$ , as

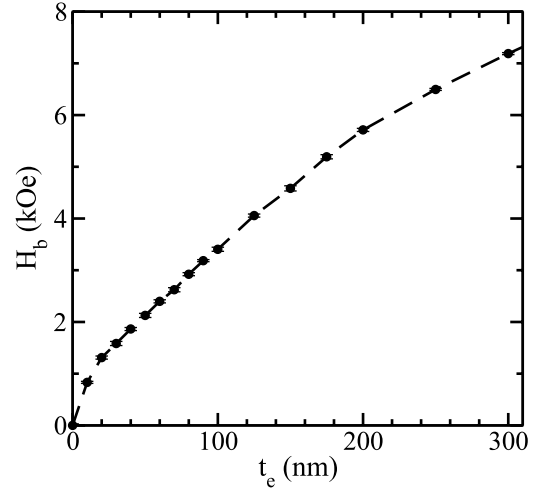
$$H_b = \frac{H_{c+} + H_{c-}}{2}. \quad (3)$$

Figure 3 shows the behavior of  $H_b$  for  $t_e$  ranging from 10 to 300 nm. We observe that, by increasing the width of the hard magnetic layer, the shift of the hysteresis loop increases following the power law  $H_b = ct_e^\gamma$ , with  $c = 0.2$  and  $\gamma = 0.63$ .

For the loop width we define the relative width variation,  $\Delta$ , as

$$\Delta = |H_c - H_{c0}|, \quad (4)$$

where  $H_{c0}$  is the average coercive field of the isolated inner wire, that is  $H_{c0} = (H_{c0+} - H_{c0-})/2$ .  $H_c$  is the average coercive field for the inner wire in the presence of the external



**Figure 3.** Bias field as a function of the width of  $t_e$ .

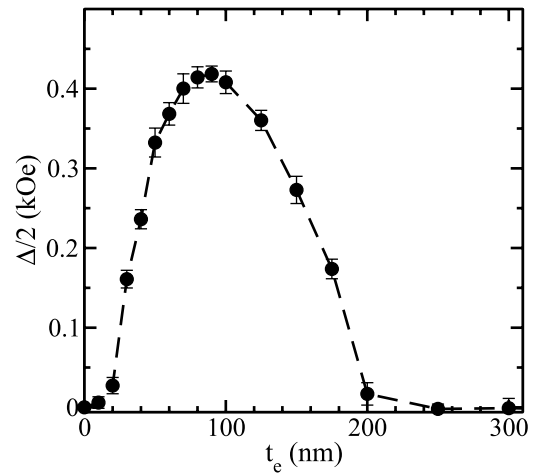


**Figure 4.** Variation of the loop width for  $t_e \neq 0$  relative to the width for an isolated wire (with  $t_e = 0$ ).

layer, defined in the same fashion as  $H_{c0}$ . Figure 4 shows a non-monotonic behavior for  $\Delta$ , with a maximum at  $t_e = 90$  nm, followed by a continuous decrease reaching the non-interacting width at  $t_e \geq 200$  nm. From the definition of  $\Delta$  it is clear that the coercivity decreases, reaching a minimum value at  $t_e = 90$  nm, and increases again up to the isolated wire value.

The asymmetry in the hysteresis loops cannot be quantified in a simple fashion. To understand its cause one has to examine the reversal process in detail. Before this, let us review the general features of the field  $\vec{H}_m^e$  due to the external layer.

Figure 5 shows a schematic representation of the field  $\vec{H}_m^e$  acting on the inner wire for an external layer magnetized in the  $+z$  direction, together with the applied field  $\vec{H}_a$ . Away from the wire tips the field is practically parallel to the cylinder axis, and its magnitude decreases towards the center of the wire. The shift in the hysteresis loop is easy to understand. If the external layer is magnetized in the  $+z$  direction the magnetic moments in the wire experience a field smaller than  $H_a$  and a

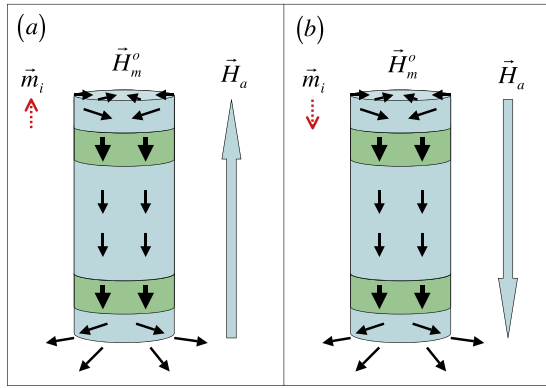


**Figure 5.** Schematic view of the field  $\vec{H}_m^e$  due to external layer acting on the inner wire. Since the external tube is made of a harder magnetic material this field may be kept constant during the hysteresis loop of the inner wire, acting as a unidirectional field. Another important characteristic of this field is its non-homogeneity. This field intensity in the central part of the inner wire is weaker than the one at the tips.

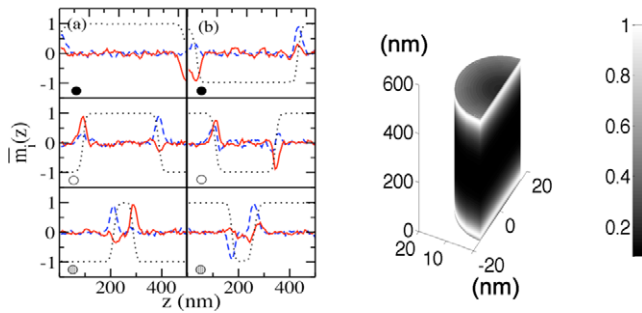


**Figure 6.** Left side: snapshots for  $t_e = 10$  nm. Right side: representation of the corresponding magnetic field.

magnetic moment in the  $+z$  direction which is inverted at a field smaller than the coercive field for the isolated wire. The opposite behavior appears for moments in the  $-z$  direction, leading to a hysteresis loop shifted to positive values of the applied field. This effect becomes stronger as  $t_e$  increases.

Variations in the reversal process are related to the non-homogeneity of  $\vec{H}_m^e$ . For the dimensions considered, the reversal occurs via domain wall propagation [15]. Domain walls nucleate non-simultaneously at the tips of the wire and propagate towards the central part. Therefore, at the beginning of the reversal process  $\vec{H}_m^e$  has a larger value than at the end, when the walls are about to meet each other. We examined this behavior by monitoring the value of  $\bar{m}_i(z) \equiv \bar{M}_i(z)/M_0$ ,  $i = x, y, z$ , which is the average value of the magnetization components at a height  $z$ , relative to the saturation value. Figures 6–8 show snapshots at six different stages of the reversal process, denoted by dots in figures 2(a), (c) and (f), together with the magnetic field due to the external layer, shown in a color scale on the right side. In these figures columns (a) and (b) correspond to the left and right branches of the hysteresis loops, respectively. This scale has been chosen such that the value 1 (white) corresponds to the maximum magnitude of  $\vec{H}_m^e$ . The dotted line represents the average axial

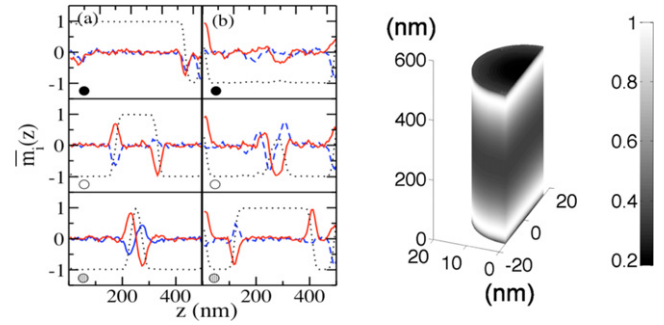


**Figure 7.** Left side: snapshots for  $t_e = 90$  nm. Right side: representation of the corresponding magnetic field.

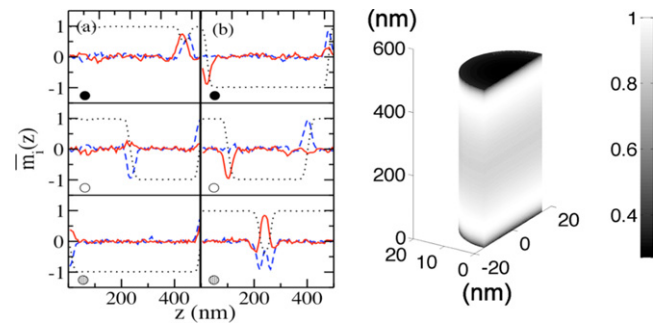


**Figure 8.** Left side: snapshots for  $t_e = 300$  nm. Right side: representation of the corresponding magnetic field.

component of the magnetization ( $\bar{m}_z$ ) while the other two (in-plane) components are given by the solid and dashed lines.

Figure 6 corresponds to  $t_e = 10$  nm and an almost symmetrical hysteresis loop. The field profile indicates a narrow region, with size comparable to the domain wall width, of strong magnetostatic field, where the domain walls nucleate. Along the rest of the wire the field is weak and varies very little. Extreme values of field are 0.08 and 1.14 kOe, leading to an overall variation around 1 kOe along the wire. Therefore, besides the shift, the hysteresis loop resembles those for the reversal of isolated nanowires [15]. For  $t_e = 90$  nm we observe a different situation. In this case we have extreme values of 0.8 and 4.8 kOe, leading to a 4 kOe variation. In the  $+z$  to  $-z$  inversion process (figure 7(a)), after the nucleation and launching, the domain walls are accelerated by a strong field. When the walls reach the central part, where the magnetostatic field is weaker, they slow down, leading to a change of the slope in the left hysteresis branch at the point illustrated with a white dot in figure 2(c). In the  $-z$  to  $+z$  inversion a different mechanism appears, since now the magnetostatic field enhances the stability of the wire magnetized in the  $-z$  direction. In this case the walls nucleated at the tips are almost static while additional walls appear at the central part of the wire, where the magnetostatic field is weaker, and propagate towards the tips.

Finally, for  $t_e = 300$  nm, the field is very intense along the tube and almost homogeneous, except for the tips, as shown in figure 8. The overall variation is about 6 kOe, but excluding the tips we observe a variation smaller than 2 kOe, although field

values are high. In the  $+z$  to  $-z$  inversion process nucleation and propagation is very fast. Notice that the propagation speed is so high that the nucleation of the second wall, at the other tip, was not observed in this specific simulation. The slowing down occurring when the walls reach the central part is not so evident in this case. In the  $-z$  to  $+z$  inversion again the wall stability is enhanced by the magnetostatic field; however, the field is almost homogeneous and so intense that the nucleation of walls in the central part is not possible. As a result the right branch of the hysteresis loop is initially rounded, corresponding to the walls moving against the stronger fields (white part), and then they are accelerated by the weaker central field.

#### 4. Discussion and conclusion

In summary, we have investigated the magnetostatic biasing effect in multilayer nanowires. Using Monte Carlo simulations we obtained the hysteresis loops of a wire covered by an external magnetic shell of varying width. Our results show a shift of the hysteresis loop towards positive fields due to the dipolar interaction between the wire and the magnetic shell, which is also observed in multilayer microwires [4]. This bias field generates a shift that increases with the thickness of the external shell. We also observe variations in the width of the hysteresis loop. What is interesting in this system is the non-homogeneity of the bias field. Apart from the tips the field due to the external layer is weaker in the central part such that the field experienced by the moving wall effectively changes along the reversal process. Also, the field gradient depends on  $t_e$  becoming less important as this thickness increases. Regarding the left branch of the hysteresis loop, where the bias field favors the propagation, the weaker field region may slow down the walls, generating a change of slope whenever the field reaches a small enough value as observed in the  $t_e = 90$  nm case. For  $t_e > 90$  nm the field is high enough along the wire that this effect is less pronounced, as observed in the  $t_e = 150, 200$  and  $300$  nm cases. On the right branch the bias field hinders the propagation, pinning the walls nucleated at the tips, leading to the nucleation of walls in the central part of the wire, where the field is weaker. These central walls are responsible for the inversion, as depicted in figure 7, and enhance the coercivity. As  $t_e$  increases, the field is strong enough in the central part of the wire, inhibiting the formation of the second pair of walls. In this case the coercivity again decreases, but a clear slow-down of the nucleation and propagation of walls is evidenced by the rounding of the initial part of the right branch of the hysteresis loop, as observed in figure 8.

In conclusion, the dipolar field of the external layer originates a bias of the hysteresis loop. The inhomogeneity of this field is responsible for the existence of different reversal processes, which lead to non-symmetrical hysteresis

loops. The behavior of these systems is the result of a competition between the strength of the magnetostatic field due to the external shell and its inhomogeneity. Multilayer nanowires open the possibility of controlling two parameters of the hysteresis loop, the coercivity and the bias, providing an interesting system to be explored theoretical and experimentally.

#### Acknowledgments

This work was supported by Fondecyt (Nos 1080300, 11070010, and 3090047), Millennium Science Nucleus Basic and Applied Magnetism (project P06-022F), and Financiamiento Basal para Centros Científicos y Tecnológicos de Excelencia. Monica Bahiana acknowledges support from Instituto do Milenio de Nanotecnologia (MCT/CNPq), FAPERJ, and PROSUL/CNPq.

#### References

- [1] Escrib J, Bachmann J, Jing J, Daub M, Altbir D and Nielsch K 2008 *Phys. Rev. B* **77** 214421
- [2] Pirota K, Hernández-Vélez M, Navas D, Zhukov A and Vázquez M 2004 *Adv. Funct. Mater.* **14** 266–8
- [3] Escrib J, Altbir D and Nielsch K 2007 *Nanotechnology* **18** 225704
- [4] Escrib J, Allende S, Altbir D, Bahiana M, Torrejón J, Badini G and Vázquez M 2009 *J. Appl. Phys.* **105** 023907
- [5] Vázquez M, Badini-Confalonieri G, Kraus L, Pirota K R and Torrejón J 2007 *J. Non-Cryst. Solids* **353** 763
- [6] d'Albuquerque e Castro J, Altbir D, Retamal J C and Vargas P 2002 *Phys. Rev. Lett.* **88** 237202
- [7] Vargas P, Altbir D and d'Albuquerque e Castro J 2006 *Phys. Rev. B* **73** 092417
- [8] Cullity B D 1972 *Introduction to Magnetic Materials* (Reading, MA: Addison-Wesley)
- [9] Mejía-López J, Altbir D, Romero A H, Batlle X, Roshchin Igor V, Li Chang-Peng and Schuller Ivan K 2006 *J. Appl. Phys.* **100** 104319
- [10] Landeros P, Allende S, Escrib J, Salcedo E, Altbir D and Vogel E E 2007 *Appl. Phys. Lett.* **90** 102501
- [11] Bahiana M, Amaral F S, Allende S and Altbir D 2006 *Phys. Rev. B* **74** 174412
- [12] Kittel C 2004 *Introduction to Solid State Physics* (New York: Wiley)
- [13] Bertotti G 1998 *Hysteresis in Magnetism. For Physicists, Materials Scientists and Engineers* (New York, NY: Academic)
- [14] Binder K and Heermann D W 2002 *Monte Carlo Simulation in Statistical Physics* (New York: Springer)
- [15] Wernsdorfer W, Doudin B, Mailly D, Hasselbach K, Benoit A, Meier J, Ansermet J-Ph and Barbara B 1996 *Phys. Rev. Lett.* **77** 1873–6
- [16] Nowak U, Chantrell R W and Kennedy E C 2000 *Phys. Rev. Lett.* **84** 163